Journal of Solid Mechanics Vol. 7, No. 4 (2015) pp. 442-457

The Effect of Fiber Breakage on Transient Stress Distribution in a Single-Lap Joint Composite Material

M. Shishehsaz [1,*], S. Yaghoubi

[1]Department of Mechanical Engineering, Shahid Chamran University, Ahwaz, Iran
[2]Department of Mechanical Engineering, Bu-Ali Sina University, Hamadan, Iran

Received 30 July 2015; accepted 5 October 2015

ABSTRACT

In the present study, the transient stress distribution caused by a break in the fibers of an adhesive bonding is investigated. Transient stress is a dynamic response of the system to any discontinuity in the fibers from detachment time till their equilibrium state (or steady state). To derive the governing dynamic equilibrium equations shear lag model is used. Here, it is assumed that the tensile load is supported only by the fibers. Employing dimensionless equations, initial conditions and proper boundary conditions, the differential-difference equations are solved using explicit finite difference method and the transient stress distribution is obtained in the presence of discontinuities. The present work aims to investigate the transient stress distribution in a single-lap joint, caused by the fiber breakage in a single layer of the adhesive joint. For this purpose, the effect of different number of broken fibers (including mid fiber) in the adherend on load distribution in other intact filaments, the location of fiber breaks in the adherend, and the effect of adhesive length is studied on the overall joint behavior. The results show that a the fiber is broken away, the amount of initial shock (maximum load) into the fiber and thus the dynamic overshoot is reduced. Maximum amount of shock in the lateral fibers is broken at this point due to breakage in the thirteenth fiber maximum axial load and shock are introduce to the fourteenth fiber.

Keywords : Composite; Fibers; Adhesive joints;, Stress concentration; Transient stress.

1 INTRODUCTION

IN engineering applications, properties combinations are often required. Since no substance can be found that have all the properties of the desired materials, we must seek another solution and the key to this problem is the use of composites. For example, in the aerospace industry, materials are required that while having high strength, they are lightweight and have good abrasion resistance. These materials are obtained by locating one or more discontinuous phase (fiber) into a continuous phase (matrix). Fiber must be having a very high tensile strength, in other words, the bulk of the force will be tolerated by the fiber [1]. In fact, the polymer matrix while protecting the physical and chemical damage transmits load to the fiber and its modulus must be lower than the fiber modules. Given the wide spread use of adhesive joints, composites in various industries, studying the behavior of these materials, particularly in the face of defects such as holes and cracks are of utmost importance.

In a structure made of composites, when any cracks or discontinuities are caused in the fiber loads must be tolerated by the fiber will be transferred through the matrix to the adjacent normal fiber that will makes stress concentration around discontinuities. Pickett et al [2] examined the elastic adhesive stresses for joints in R. F. P.

*Corresponding author. Tel.: +98 0611 3330011. ; Fax: 0611 3336642.
E-mail address: *mshishehsaz@scu.ac.ir* (M. Shishehsaz).

Structures. Unlike the work done in the past, which mostly considered the solution of closed form of adhesive stress distribution in joints, in this study, two classical technique and the theory of finite element to analyze the stress distribution in single-lap, two-lap and pipe-shaped joints are used. When using classical analysis, solving the derived governing differential equations require a numerical method which here the procedures has been expressed for when the finite difference numerical method is used. The results showed the agreement and overlapping of responses obtained from the two methods. Nedel et al [3] have examined the coefficient of stress concentration near a broken fiber in a single carbon–Epoxy composite. Its symmetry-oriented analysis showed that the stress concentration factor for all modes in the adjacent fiber is predicted less than 1.10 by Hedgepeth. Rajabi et al [4] have examined the effects of stress concentration in the single-lap adhesive joints of composites using ABAQUS. The results of this modeling showed that significant changes in stresses occur in the thickness of the adhesive layer near the end of joint length. Wang et al [5] using experimental results and the finite difference method, have examined the distribution of stress - strain around the trailing edges overlapping in a single - lap joint made of the composite material. The results showed that a remarkable overlapping exists between the finite element results and experimental results. Beylergil et al [6] conducted a numerical and experimental analysis on composite single-lap joints whose research was done for two types of joints. The first type, the normal and traditional single-lap joint without adhesion and in the type II, fiber rods were also considered. The results showed that the fiber improved the ultimate strength and time accuracy of joint damage and these experimental results have an acceptable overlapping with the numerical results. Challita et al [7] have offered an analytical model for double-lap joints for the response to the harmonic forces. The model considered is based on the improved model of Shear-Lag, and they compared the simple and improved mode of Shear-Lag with the finite element model. The results showed that the improved Shear-Lag model is closer than other models to the finite element model. Mokhtari et al [8] have investigated the effect of layer stiffness, its thickness as well as fibers being multi-direction on the stress distribution in two lap adhesive joining by applying three-dimensional finite element analysis in ABAQUS. In this modelling, the nonlinear behavior of the adhesive is also considered and six laminated with different orientation of the fiber were used which composite material made from Carbon-Epoxy, Bern-Epoxy, Graphite-Epoxy and Aramid - Epoxy. Results of the modeling showed that with changes in stiffness and the direction of the fibers in the material, the maximum stress was significantly reduced and the shear stress can be reduced using hybrid composites.

Mousavitabar [9] has examined the compound single-lap joint located on the tensile edge. In this work, in addition to the shear stress generated in the adhesive layer, the distribution of axial load in single layers is also examined. The analysis conducted in this paper is based on the Shear-Lag theory and modified Shear-Lag and ultimately the values extracted from the solution were compared with the values obtained from numerical software ANSYS. The results showed that in the composites where the elasticity modulus of the matrix is lower, the values obtained has a proper overlapping with numerical solution, but when modulus of the matrix is high, the theory of modified Shear-Lag suggests detailed answer than Shear-Lag theory. Daniali [10] has calculated the values of stress concentration factor for both single-layer and double-multilayer adhesive joints in the cracks existence. The results showed that the cracks existence create the maximum shear stress concentration in the adhesive layer neighboring the middle of crack edges and the maximum concentration of tensile stress in the fiber at the crack tip.

If in a joint made from composite materials, one or more fiber is broken, after a certain time, the joint reaches equilibrium. From the moment of detachment of fibers to before the moment of balance in it, transient stress distribution in the desired structure is created. To obtain the static and dynamic stress concentration factor in a single layer with infinite dimensions made of composite material, Hadgepath [11] extracted relationships based on the Shear-Lag theory. Then, he used a solution similar to the static solution for dynamic modes, but due to the solution complexity he could not solve the equations for more than three broken fibers. Mirshekari [12] has obtained the transient stress distribution in a variety of composites influenced by crack. Results showed that increasing the number of broken fiber, stress concentration factor increases in composite material.

As explained in the overview of research, studies conducted in the field of transient stresses are only related to the single layer and multilayer composites. Purpose of this study is to investigate the transient stress distribution caused by fiber breakage in a single layer number one in single-lap adhesive joint. For this work, the effect of different numbers of fiber breakage on the adhesive joint, the impact of displacement of starting point of discontinuity in the perpendicular on fibers, impact of adhesive and non-adhesive changes of length on composite material and finally the effect of changes of the distance between the fiber on adhesive joint behavior have been studied.

2 THEORITICAL FOUNDATION OF TRANSIENT STRESS DISTRIBUTION IN ADHESIVE JOINT

In tensile single-lap adhesive joint, two single-layers are connected by an adhesive layer and the tensile load applied on the edges is static. Since the load applied from either side is not located on one direction, bending stress is created and caused by the unevenness. This bending is ignored in this research. In Fig. 1, a single-lap joint made of the composite material can be seen in two single layers are connected by the adhesive layer. As indicated in Fig.1, the discontinuity is created in adhesive area of one of the single-layers and in single-layer number one.

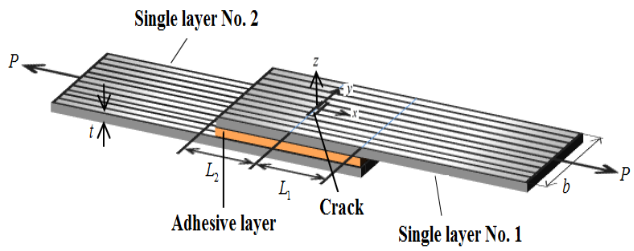

Fig.1
Single-lap composites bonding in presence of adhesive layer.

In Fig. 2, the two-dimensional deformed view of the adhesive bonding is shown.

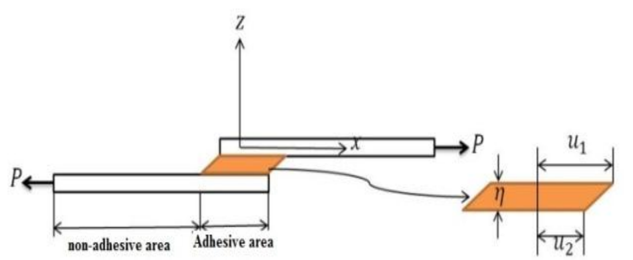

Fig.2
Figure of adhesive bonding on $x-z$ page and deformed model of adhesive.

Using the definition of shear stress, Eq. (1) is extracted for the shear stress applied to the fiber from the adhesive layer. In this regard, G is the shear modulus of the adhesive layer, η thickness of the adhesive layer, u_1 axial place shift in single-layer number one and u_2 axial place shift in a single layer number two.

$$\tau_{zx} = G\cdot(\gamma_{zx}) = G\cdot(\cancel{\frac{\partial w}{\partial x}} + \frac{\partial u}{\partial z}) = G\cdot\frac{\partial u}{\partial z} = G\cdot(\frac{u_1 - u_2}{\eta}) \tag{1}$$

Due to the amount of displacement along *y* and *z* against the displacement amount is negligible along *x*, so in this equation, the change of displacement along *z* than *x* are ignored and replacement is assumed linear in direction with the adhesive layer thickness.

2.1 Extracting the equations governing the adhesive region

The purpose of this chapter is to derive the displacement of fibers differential equations in single layer number one and two. In Fig. 3, the free-body diagram of fiber elements number n and matrix between fiber number n and $n-1$ in the single-layer adhesive region number one and two is given.

It should be noted that in Fig. 3, d_f, d_m, τ_{zx} and τ'_{zx} are respectively the fiber thickness, matrix thickness, shear stress exerted on the fibers and the matrix from the adhesive layer.

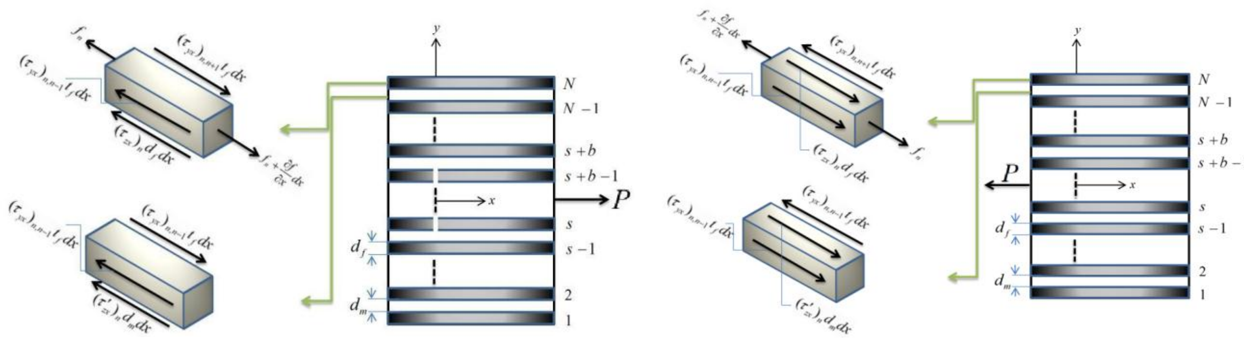

(a) (b)

Fig.3
Free-body diagram of a single-layer in adhesive area. a) single-layer numbers one, b) Single Layer Number two.

Shear stress imposed by the adhesive cause applying a shear force on the matrix. This is due to assuming the displacement in matrix linear, the shear stress τ_{yx} is proved in it, so this force is divided equally between the two fibers connected to the matrix. In Eq. (2), how to transfer the shear force has been expressed. In this equation, $(F_1)_n$ represents the force transferred from the matrix to the fiber and u_n, v_n, u'_n and v'_n are the displacement of the fiber and matrix number n in the single layer number one and two respectively.

$$
\begin{aligned}
(F_1)_n &= \left[\frac{1}{2}(\tau'_{zx})_n + \frac{1}{2}(\tau'_{zx})_{n-1}\right]\cdot d_m \cdot dx = \frac{G}{\eta}\cdot\left[\frac{(u'_{n-1}+u'_n)}{2} - \frac{(v'_n+v'_{n-1})}{2}\right]\cdot d_m \cdot dx = \\
&\frac{G}{\eta}\cdot\begin{bmatrix}\frac{1}{2}\left(\frac{(u_n+u_{n-1})}{2}+\frac{(u_n+u_{n+1})}{2}\right)- \\ \frac{1}{2}\left(\frac{(v_n+v_{n-1})}{2}+\frac{(v_n+v_{n+1})}{2}\right)\end{bmatrix}\cdot d_m \cdot dx = \frac{1}{2}\left[(\tau_{zx})_n + \frac{1}{2}(\tau_{zx})_{n-1} + \frac{1}{2}(\tau_{zx})_{n+1}\right]\cdot d_m \cdot dx
\end{aligned} \tag{2}
$$

In equation obtained, the displacement changes in matrix in the direction x are assumed linear relative to y. Due to the shear stress induced by the adhesive layer in connecting with the fiber, a force is imposed on it equal to $(\tau_{zx})_n \cdot d_f \cdot dx$, so the equivalent force from the adhesive on the fiber n can be achieved from the sum of these forces and transferred forces as Eq. (3).

$$
F_n = (\tau_{zx})_n \cdot d_f \cdot dx + (F_1)_n = (\tau_{zx})_n \cdot (d_f + \frac{1}{2}d_m)\cdot dx + \frac{1}{4}(\tau_{zx})_{n-1}\cdot d_m \cdot dx + \frac{1}{4}(\tau_{zx})_{n+1}\cdot d_m \cdot dx \tag{3}
$$

with applying desired changes in the force imposed on the fiber and matrix, shear force exerted by the adhesive is removed from the matrix and finally the two-dimensional free-body mode of fiber and matrix is obtained as in Fig. 4. According to this figure, the dynamic equilibrium equation along x for single layer adhesive region of fiber number one can be expressed as Eq. (4).

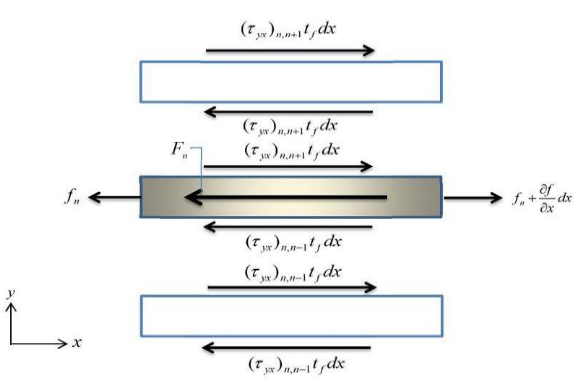

Fig.4
Free-body diagram of the fiber and matrix in a single layer adhesive area number one after force transmission from matrix to the fiber.

$$\sum f_x = m\cdot dx\cdot \ddot{u} \Rightarrow f_n + \frac{\partial f_n}{\partial x}\cdot dx + (\tau_{yx})_{n+1,n}\cdot t_f\cdot dx - f_n - F_n - (\tau_{yx})_{n,n-1}\cdot t_f\cdot dx = m\cdot dx\cdot \ddot{u}_n \tag{4}$$

In Eq. (4), m is the mass per length of the fiber, $(\tau_{yx})_{n+1,n}$ is the shear stress imposed by the matrix which is located between fiber number $n+1$ and n Shear stress applied to the fiber from the matrix will be obtained respectively, from the Eqs. (5) and (6) by considering a linear shift in it and the tensile force in the fiber with its axial displacement.

$$\tau_{yx} = G_m\cdot(\gamma_{yx}) = G_m\cdot(\cancel{\frac{\partial \upsilon}{\partial x}} + \frac{\partial u}{\partial y}) = G_m\cdot\frac{\partial u}{\partial y} \tag{5}$$

$$f_n = \sigma_n\cdot A_n = E_n\cdot\varepsilon_n\cdot A_n = E_n\cdot A_n\cdot\frac{\partial u}{\partial x} \tag{6}$$

Due to the shift in the linear matrix, it is assumed that the shear stress exits imposed by the fiber matrix number $n+1$ and n will be extracted from the Eq. (7).

$$(\tau_{yx})_{n+1,n} = \frac{G_m}{d_m}\cdot(u_{n+1} - u_n) \tag{7}$$

Using Eqs. (1), (3), (6) and (7), Eq. (4) (which represents the dynamic equilibrium equations of fibers in single-layer adhesive areas number one) is rewritten in terms of displacement of fibers as the Eq. (8).

$$\begin{aligned}
&E_n\cdot A_n\cdot(\frac{\partial^2 u_n}{\partial x^2}) + \frac{G_m\cdot t_f}{d_m}\cdot(u_{n+1} - 2u_n + u_{n-1}) + \frac{G\cdot(d_f + 0.5d_m)}{\eta}\cdot(v_n - u_n) + \frac{1}{4}\frac{G\cdot(d_m)}{\eta}\cdot(v_{n-1} - \\
&u_{n-1}) + \frac{1}{4}\frac{G\cdot(d_m)}{\eta}\cdot(v_{n+1} - u_{n+1}) = m\cdot\frac{\partial^2 u_n}{\partial t^2} \qquad 2\le n\le N-1 \\
&E_1\cdot A_1\cdot(\frac{\partial^2 u_1}{\partial x^2}) + \frac{G_m\cdot t_f}{d_m}\cdot(u_2 - u_1) + \frac{G\cdot d_f}{\eta}\cdot(v_1 - u_1) + \frac{1}{2}\frac{G}{\eta}\cdot(\frac{(v_2 + v_1)}{2} - \frac{(u_2 + u_1)}{2})\cdot d_m = m\cdot\frac{\partial^2 u_1}{\partial t^2} \\
&E_N\cdot A_N\cdot(\frac{\partial^2 u_N}{\partial x^2}) + \frac{G_m\cdot t_f}{d_m}\cdot(u_{N-1} - u_N) + \frac{G\cdot d_f}{\eta}\cdot(v_N - u_N) + \frac{1}{2}\frac{G}{\eta}\cdot(\frac{(v_N + v_{N-1})}{2} - \frac{(u_N + u_{N-1})}{2})\cdot d_m = m\cdot\frac{\partial^2 u_N}{\partial t^2}
\end{aligned} \tag{8}$$

Since two free edge fibers are in close proximity of a matrix, so the differential equation governing the two is different from the rest of the fibers in each layer. In Eq. (8), u represents the displacement along x for fiber existing in single layer number one and v represents the displacement in x direction for existing fibers in single-layer number two. With a procedure the same as the previous section, the dynamic equilibrium equations are extracted for a single layer, number two in Eq. (9).

$$\begin{aligned}
&E_n\cdot A_n\cdot(\frac{\partial^2 v_n}{\partial x^2}) + \frac{G_m\cdot t_f}{d_m}\cdot(v_{n+1} - 2v_n + v_{n-1}) - \frac{G\cdot(0.5d_m + d_f)}{\eta}\cdot(v_n - u_n) - \frac{1}{4}\frac{G\cdot d_m}{\eta}\cdot(v_{n-1} - \\
&u_{n-1}) - \frac{1}{4}\frac{G\cdot d_m}{\eta}\cdot(v_{n+1} - u_{n+1}) = m\cdot\frac{\partial^2 v_n}{\partial t^2} \qquad 2\le n\le N-1 \\
&E_1\cdot A_1\cdot\frac{\partial^2 v_1}{\partial x^2} + \frac{G_m\cdot t_f}{d_m}\cdot(v_2 - v_1) - \frac{G\cdot d_f}{\eta}\cdot(v_1 - u_1) + \frac{1}{2}\frac{G}{\eta}\cdot(\frac{(u_2 + u_1)}{2} - \frac{(v_2 + v_1)}{2})\cdot d_m = m\cdot\frac{\partial^2 v_1}{\partial t^2} \\
&E_N\cdot A_N\cdot(\frac{\partial^2 v_N}{\partial x^2}) + \frac{G_m\cdot t_f}{d_m}\cdot(v_{N-1} - v_N) - \frac{G\cdot d_f}{\eta}\cdot(u_N - v_N) + \frac{1}{2}\frac{G}{\eta}\cdot(\frac{(u_N + u_{N-1})}{2} - \frac{(v_N + v_{N-1})}{2})\cdot d_m = m\cdot\frac{\partial^2 v_N}{\partial t^2}
\end{aligned} \tag{9}$$

In adhesive areas, due to the existence of shear stress caused by adhesives, fibers dynamic equilibrium differential equations in two single-layer numbers one and two are interdependent and must be solved simultaneously. The number of equations obtained for the adhesive area is $2N$.

2.2 Making the equations governing the adhesive areas dimensionless

A series of dimensionless parameters used in Eqs. (10) to (18) have been introduced in making the differential equations of displacement of the adhesive area dimensionless.

$$\xi = \frac{x}{\lambda} \tag{10}$$

$$\tau = \frac{t}{T} \tag{11}$$

$$T = \sqrt{\frac{m}{E_f \cdot A_f}} \cdot \lambda \tag{12}$$

$$F_n = \frac{f}{p} \tag{13}$$

$$\phi_1 = \frac{\lambda^2 \cdot G_m \cdot t_f}{E_f \cdot A_f \cdot d_m} \tag{14}$$

$$\phi_2 = \frac{\lambda^2 \cdot G \cdot d_f}{E_f \cdot A_f \cdot \eta} \tag{15}$$

$$\phi_3 = \frac{\lambda^2 \cdot G \cdot d_m}{4E_f \cdot A_f \cdot \eta} \tag{16}$$

$$\phi_4 = \frac{\lambda^2 \cdot G}{E_f \cdot A_f \cdot \eta}(d_f + 0.5d_m) \tag{17}$$

$$S_{xy} = \frac{E_f \cdot A_f \cdot d_m}{G \cdot p \cdot \lambda} \cdot \tau_{xy} \tag{18}$$

Closed dimensionless form of equations governing the adhesive area is as Eq. (19).

$$E \cdot W'' - L \cdot W = M \cdot \ddot{W} \tag{19}$$

where the vector $w,\ w''$ and $\ddot{w}$ are defined as Eqs. (20) to (22) respectively.

$$W = \{U_1, U_2, \dots, U_N, V_1, V_2, \dots, V_N\}_{2N\times 1} \tag{20}$$

$$W'' = \{U_1'', U_2'', \dots, U_N'', V_1'' V_2'', \dots, V_N''\}_{2N\times 1} \tag{21}$$

$$\ddot{W} = \{\ddot{U}_1, \ddot{U}_2, \dots, \ddot{U}_N, \ddot{V}_1, \ddot{V}_2, \dots, \ddot{V}_N\}_{2N\times 1} \tag{22}$$

Matrixes M and E existing in Eq. (19) are unit matrixes to dimensions $2N \times 2N$. Due to the different algorithms of side fibers with other fibers are extracted with writing the first three sentences for each single layer matrix L as Eq. (23).

$$L = \begin{Bmatrix} L_1 & L_2 \\ L_3 & L_4 \end{Bmatrix} \tag{23a}$$

$$L_1 = L_4 = \begin{bmatrix} \phi_1+\phi_2+\phi_3 & -\phi_1+\phi_3 & 0 & \cdots & 0 \\ -\phi_1+\phi_3 & 2\phi_1+\phi_4 & \ddots & \ddots & \vdots \\ 0 & \ddots & \ddots & \ddots & 0 \\ 0 & 0 & \ddots & 2\phi_1+\phi_4 & -\phi_1+\phi_3 \\ 0 & \cdots & 0 & -\phi_1+\phi_3 & \phi_1+\phi_2+\phi_3 \end{bmatrix}_{N\times N} \tag{23b}$$

$$L_2 = L_3 = \begin{bmatrix} -\phi_2-\phi_3 & -\phi_3 & 0 & \cdots & 0 \\ -\phi_3 & -\phi_4 & \ddots & 0 & \vdots \\ 0 & \ddots & \ddots & \ddots & 0 \\ \vdots & 0 & \ddots & -\phi_4 & -\phi_3 \\ 0 & \cdots & 0 & -\phi_3 & -\phi_2-\phi_3 \end{bmatrix}_{N\times N} \tag{23c}$$

where L_1 to L_4 each are matrix $N \times N$ and are defined as follows.

2.3 Deriving the equations governing non-adhesive parts

In non-adhesive areas, there is no shear stress due to adhesive and since the shear stress of displacement links the single layer of fibers number one and two together, so in this region solving the differential equations of two single-layer displacement is independent from each other. With the same trend as adhesive region, closed and dimensionless form of dynamic equilibrium equations number one and two are given respectively, in the relations (24) and (25).

$$E'\cdot U'' - L'\cdot U = M'\cdot \ddot{U} \tag{24}$$

$$E'\cdot V'' - L'\cdot V = M'\cdot \ddot{V} \tag{25}$$

where the matrixes E' and M' are unit matrix of dimensions $N \times N$, using dimensionless parameters introduced, the matrix L' is obtained from the Eq. (26).

$$L' = \begin{bmatrix} \phi_1 & -\phi_1 & 0 & 0 & 0 & \cdots & 0 \\ -\phi_1 & 2\phi_1 & -\phi_1 & 0 & 0 & \cdots & 0 \\ 0 & -\phi_1 & 2\phi_1 & -\phi_1 & 0 & \cdots & 0 \\ 0 & \ddots & \ddots & \ddots & \ddots & \ddots & \vdots \\ 0 & \cdots & 0 & -\phi_1 & 2\phi_1 & -\phi_1 & 0 \\ \vdots & 0 & \cdots & 0 & -\phi_1 & 2\phi_1 & -\phi_1 \\ 0 & 0 & 0 & \cdots & 0 & -\phi_1 & \phi_1 \end{bmatrix}_{N\times N} \tag{26}$$

2.4 Initial conditions and boundary conditions

Initial conditions in adhesive bonding include two stages before rupture and the moment of discontinuity in fiber. Initial conditions before the discontinuity is such that the load in all fibers is equal to P (Tensile load applied to the fiber away from the discontinuity) and the dimensionless form of the initial condition is expressed in Eq. (27).

$$P_n(\xi,0)=1 \tag{27}$$

The next initial condition is the discrete time of fiber that at this point, each fiber is at rest and its instantaneous velocity is considered as Eq.(28).

$$\frac{\partial U_n}{\partial \tau}(\xi,0)=0 \tag{28}$$

Boundary conditions are related to the moment after detachment of fibers which for normal and broken fibers two quite distinct conditions are established. In detached fibers, the boundary conditions are such that the force exerted on them at the location of the detachment is equal to zero and is expressed as relation (29).

$$P_n(0,\tau)=0 \qquad (s\le n\le s+b-1) \tag{29}$$

In Eq. (29), dislocation is started from the fiber s and the number of detached fibers is equal to b. In normal fibers, the situation is different. According to the fact that the dimensionless load on the right edge is equal to one and on the left edge is equal to zero, using the backward difference form at the edge of imposing load and the form of leading difference in free edge, initial displacement of normal fibers are obtained at the point where is the same length of the discontinuity place.

2.5 Solving the governing differential equations

As it is obvious from the relations (19), (24) and (25), fiber displacement differential equation is second-order and with two variables. To solve the differential equation obtained, the explicit finite difference method is used [13]. Due to the fact that the displacement values in addition to place are also dependent to the time, overall the fiber displacement vector is expressed as $u_n^{i,j}$ in which terms subtitle n expresses the fiber number and superscripts i and j represent the number of displacement step and time step respectively [14].

In adhesive area, since the displacement of two single layers is related to each other, so the differential equations must be solved simultaneously. For solving differential equations, adhesive area are divided into two parts of separate right and left discontinuities that finally by applying the boundary conditions at detachment place of the fiber, two single-layer adhesive area displacements is obtained in form of vector w. Considering the form of central difference form for the second displacement and time derivative, Eq. (19) can be expressed as Eq. (30) to calculate the amount of displacement in the new time period.

$$W_n^{i,j+1}=-\frac{(\Delta\tau)^2}{M_{n,n}}\sum_{k=1}^{2N}L_{n,k}\cdot W_k^{i,j}+2(1-(\frac{\Delta\tau}{\Delta\xi})^2\cdot(\frac{E_{n,n}}{M_{n,n}}))\cdot W_n^{i,j}+(\frac{\Delta\tau}{\Delta\xi})^2\cdot(\frac{E_{n,n}}{M_{n,n}})\cdot(W_n^{i+1,j}+W_n^{i-1,j})-W_n^{i,j-1} \tag{30}$$

To calculate the $w_n^{i,j}$ and $w_n^{i,j-1}$, the initial conditions and for calculating $w_n^{i-1,j}$, boundary conditions are used. Considering these conditions, the displacement vector in the first and second spatial step are obtained as the the Eqs. (31) and (32).

$$W_n^{2,1}=W_n^{1,1}+\Delta\xi,\ldots,W_n^{2N,1}=W_n^{2N-1,1}+\Delta\xi \qquad 1\le n\le 2N \tag{31}$$

$$W_n^{i,2}=W_n^{i,1} \qquad 1\le n\le 2N \tag{32}$$

Using the initial and boundary conditions, the amount of displacement of the fibers in the first spatial step is extracted from the Eqs. (33) and (34).

$$W_n^{1,j+1} = -\frac{(\Delta\tau)^2}{M_{n,n}}\sum_{k=1}^{2N} L_{n,k}\cdot W_k^{1,j} + 2(1-(\frac{\Delta\tau}{\Delta\xi})^2\cdot(\frac{E_{n,n}}{M_{n,n}}))\cdot W_n^{1,j} + (\frac{\Delta\tau}{\Delta\xi})^2\cdot(\frac{E_{n,n}}{M_{n,n}})\cdot(W_n^{2,j} + W_n^{0,j}) - W_n^{1,j-1}$$
$$(1 \le j \le S_t) \quad (n < s \quad or \quad n > s+b-1) \tag{33}$$

$$W_n^{1,j+1} = -\frac{(\Delta\tau)^2}{M_{n,n}}\sum_{k=1}^{2N} L_{n,k}\cdot W_k^{1,j} + 2(1-(\frac{\Delta\tau}{\Delta\xi})^2\cdot(\frac{E_{n,n}}{M_{n,n}}))\cdot W_n^{1,j} + 2(\frac{\Delta\tau}{\Delta\xi})^2\cdot(\frac{E_{n,n}}{M_{n,n}})\cdot W_n^{2,j} - W_n^{1,j-1}$$
$$(1 \le j \le S_t) \quad (s \le n \le s+b-1) \tag{34}$$

where S_t is the number of time steps.

Using relations (31) and (32), the displacement values are obtained in two first time stages. To calculate the amount of displacement from the third time on, if $i=1$, the relations (33) and (34), and otherwise, the fiber displacement values are obtained from the Eq. (30). Non-adhesive single-layer displacement vectors number one and two are also extracted the same as the trend of adhesive area.

2.6 Calculating the stress concentration factor and shear stress

Stress concentration in composite materials is defined as the ratio of load to the first normal fiber following the discrete fibers in the place of creating discontinuities ($P_{f_n+b_r}^{(1,j)}$) to the load on the same fiber and at a distance away from the location of the discontinuity (in case of dimensionless it is equal to one) and its dimensionless form is expressed as the relation (35).

$$K_r = P_{f_n+b_r}^{(1,j)} = \frac{\partial U_{f_n+b_r}^{(1,j)}}{\partial\xi} = \frac{U_{f_n+b_r}^{(2,j)} - U_{f_n+b_r}^{(1,j)}}{\Delta\xi} \tag{35}$$

In Eq. (35), the index $f_n + b_r$ represents the number of desired fiber.

Dimensionless form of shear stress in the matrix where the above and down fibers are normal and are placed before discrete fibers is calculated from the relation (36).

$$S_{xy} = U_{f_n-1}^{(2,j)} - U_{f_n-2}^{(2,j)} \tag{36}$$

To calculate the shear stress generated in the adhesive, the same longitude points of two fibers are used as in single layer number one and two as in Eq. (37).

$$S'_{xy} = U_{f_n}^{(2,j)} - V_{f_n}^{(2,j)} \tag{37}$$

The ratio of maximum stress concentration factor to stress concentration factor in the static mode are called dynamic overshoot which is shown with η_r . The parameter is calculated in Eq. (38).

$$\eta_r = \frac{\max(K_r)}{(K_r)_s} \tag{38}$$

where $(K_r)_s$ is the stress concentration factor in static mode.

3 RESULTS

Calculating the stress concentration factor, axial load and shear stress in the adhesive joint requires the adhesive composites properties and adhesive that in this study, the desired composite material has a fiber made of glass and matrix made of epoxy and the values in Table 1. is used for extracting graphs.

Table 1
Mechanical properties of composite and adhesives used.

Type of material	Material	Modulus of elasticity (*GPa*)
Fiber	Glass	74
Matrix	Epoxy	1.28
Adhesive	Epoxy phenolic	1.11

In single layer modeling and connectivity, a geometry is intended which specification is given in Table 2.

Table 2
The geometry of the desired compound.

Specifications	Size
Length of each layer	250 mm
Length of overlapping area	50 mm
Layer thickness	0.1 mm
Thickness of the adhesive	0.1 mm
Fiber and matrix width	0.1 mm
load applied to each edge	100 Newton
The number of fibers in each single layer	25

Since in reference [11], the values of static stress concentration factor for cases where there is discontinuity in the middle of a single-layer composite, therefore, to verify the solution method, we first review the results of this case. In Fig. 5, the stress concentration factors is drawn for the case of fiber discrete is traced from the middle of single-layer.

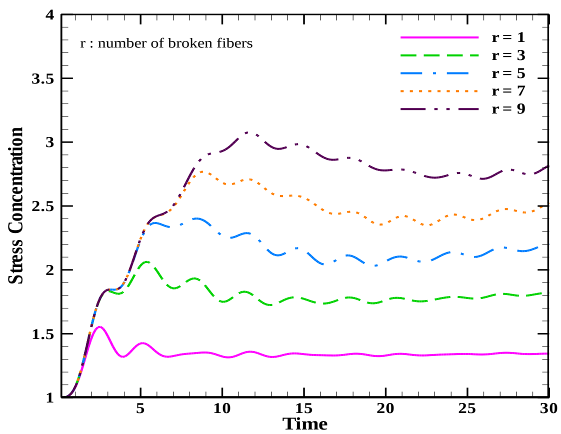

Fig.5
Diagram of stress concentration factor n terms of time in a single layer, for a condition that the discontinuity is created in the middle of the plate.

In Table 3., the static and dynamic stress concentration factor (the maximum value of stress concentration factor) obtained in Fig.5 are given.

Table 3
Results of single-layer discontinuity in the middle of the plate.

The number of broken fiber	Dynamic stress concentration factor	The converged value	Static stress concentration factor [11]	Rate of method difference
1	1.55	1.34	1.33	0.75%
3	2.06	1.82	1.83	0.54%
5	2.40	2.21	2.22	0.45%
7	2.77	2.53	2.55	0.78%
9	3.08	2.82	2.84	0.71%

As it is clear from Table 3., the values of converged stress concentration factor are significantly overlapped with static stress concentration factor values extracted from reference [11], thus this result is confirming the accuracy of the numerical method used in this research. In Fig. 5, to demonstrate the accuracy of the solution, the dimensionless unit is considered as 30 units. Since some of the figures depicted in the next sections, the difference between the curves is negligible, so for more clarity in rest of diagrams, the dimensionless time is considered equal to 15 units.

The purpose of this section is to examine the results of composite single-lap in adhesive joint. To derive the equations governing adhesive joint, the reference [10] is used and the results obtained for composite structures are based on the values in Table 1. and Table 2. In Fig. 6, the graph of axial load applied to the crack tip fiber (fiber discrete) for different numbers of discrete fibers is shown for a state where the discontinuity is created in the middle of the adhesive area. The curves obtained indicate that increasing the number of discrete fibers, the axial load applied to the fiber, and as a result the stress concentration factor in adhesive joint also increases.

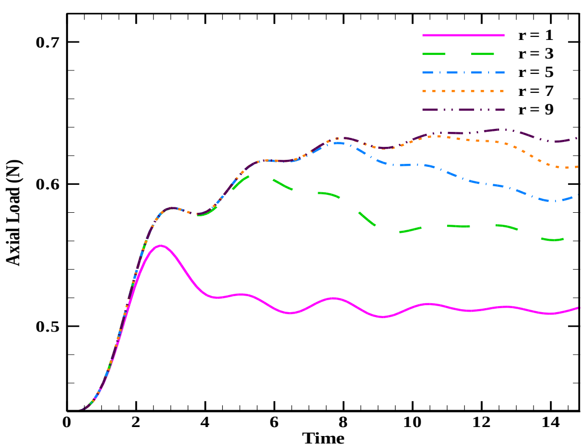

Fig.6
Diagram of the axial load applied to the fiber in connection for a discontinuity in the middle of the adhesive area.

In Table 4., the maximum load applied to the fiber at the tip of the discontinuity location is provided for single-layer composite and adhesive joint.

Table 4
The maximum load applied to the fiber in tip of discontinuity location for lamina and adhesive joint.

The number of broken fiber	Crack-tip fiber in adhesive joint (N)	Crack-tip fiber in lamina (N)
1	0.557	6.243
3	0.607	8.249
5	0.629	9.645
7	0.637	11.082
9	0.639	12.321

From the diagrams in Fig. 6 and maximum values of the axial load applied to the fibers in a single layer and adhesive joint given in Table 4., it can be concluded that in adhesive joint a remarkable amount of loads applied to fiber are absorbed by the adhesive. As a result of it, the amount of axial load and the stress concentration factor in adhesive joint composite are too low.

In Table 5., the values of dynamic overshoot are given using Eq. (38) for three fractures of fiber in a single layer and adhesive joint and their values were compared.

Table 5
Dynamic overshoot values in a single layer and adhesive joint.

The number of broken fiber	The amount of dynamic overshoot in single-layer	The amount of dynamic overshoot in adhesive joint
1	1.156	1.089
3	1.133	1.077
5	1.089	1.071

The values obtained from Table 5. indicate that the amount of dynamic overshoot in single-layer is greater than adhesive joint. Due to the fact that in this connection, there is an adhesive layer, it is expected that less shock is imposed to the system by fiber breakage. By reducing the numerical distance between the values of the dynamic and static stress concentration factor, dynamic overshoot is reduced for adhesive joint to composite single-layer that the results in Table 5. indicate the problem.

The purpose of this section is investigating the effect of displacement of discontinuity start point in the direction perpendicular to the fibers. In Fig. 7, the axial load distribution in the fiber tip of crack is given for four different starting points. In all graphs, the number of broken fibers is considered one number and location of fracture in the middle of adhesive area.

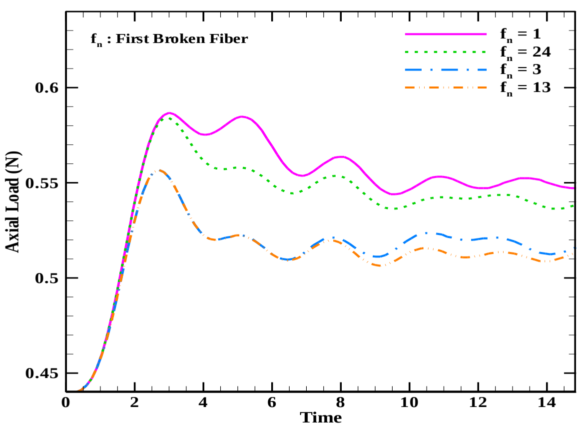

Fig.7
Diagram of load distribution in terms of time for displacement of discontinuity starting point.

In Table 6., the values of maximum load applied are given for four different starting points.

Table 6
The values of the dynamic stress concentration factor and the maximum load applied to the fiber as a result of the displacement of discontinuity starting point.

The first broken fiber	The maximum applied load (N)
1	0.587
24	0.584
3	0.557
13	0.557

The values obtained from Table 6. indicate that however the starting point of discontinuity goes to the top edge and bottom edge, the amount of load applied and as a result the stress concentration factor increases. Another point that can be obtained from this table is that distribution of load in the fibers away from the edge and close to the middle of the plate has little variation and has almost equal values.

In Fig.8 and Fig. 9, respectively, the graphs of adhesive shear stress generated in the matrix and adhesive are given for two different starting points. The diagrams obtained indicate that by taking away from the top and bottom edges, the amount of shear stress generated in the adhesive and matrix is reduced.

One of the important factors in the stress distribution of joint is the adhesive and non-adhesive zone length change which is discussed in this section and purpose is to examine the effect of length of adhesive zone on the applied load and shear stress in the matrix and adhesive. Graph of applied load to the fibers is shown in Fig. 10. It should be noted that the adhesive area are considered respectively five centimeters, eight centimeters and ten centimeters and in all three cases, the length of discontinuity is considered as constants and are assumed to have a number of broken fibers.

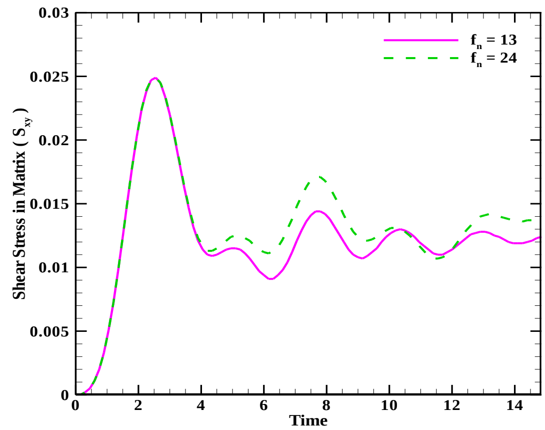

Fig.8
Diagram of shear stress in matrix for different discontinuity starting points.

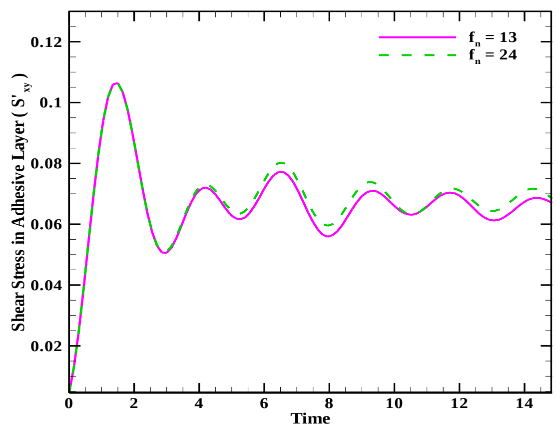

Fig.9
Diagram of shear stresses in the adhesive for different discontinuity starting points.

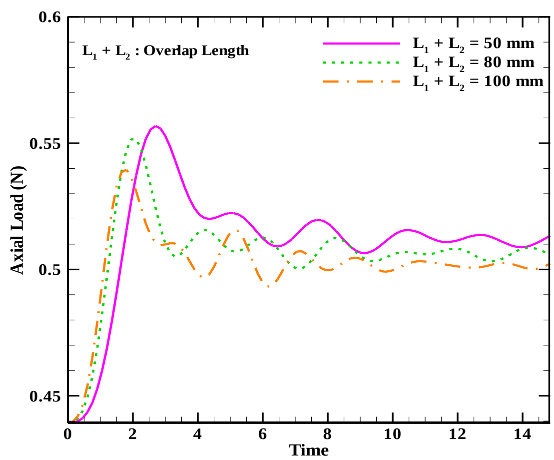

Fig.10
Diagram of the effect of changes in adhesive zone on the load applied to the fiber crack tip.

In an adhesive connection, since by increasing the adhesive area, more length of the fibers is in contact with the adhesive, so a greater amount of load applied to the fibers is absorbed by the adhesive and thereby increasing the adhesive area length, the amount of load applied to the fiber decreases. Due to the fact that stress concentration factor is related to the amount of load in the fiber tip in discontinuity location, thus reducing the load applied, this factor is also decreased which diagrams obtained from Fig. 10 illustrates this issue.

The impact of length change in the adhesive area on shear stress generated in the matrix and adhesive, are respectively shown in Figs. 11 and 12. As is clear from the graphs extracted, increasing the length of the adhesive bonding, reduces the shear stress in the matrix and adhesive like the axial load and stress concentration factor.

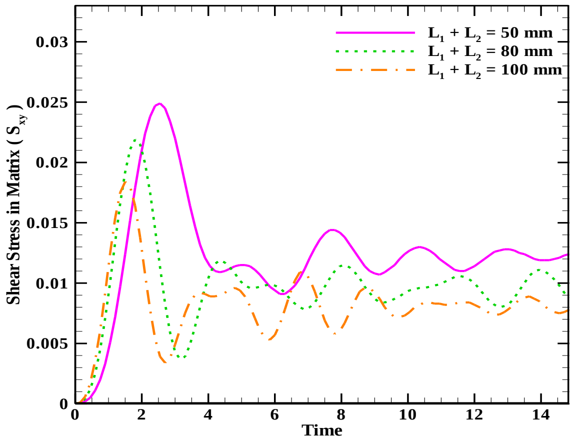

Fig.11
Diagram of the effect of the change of length in the shear stress in the matrix.

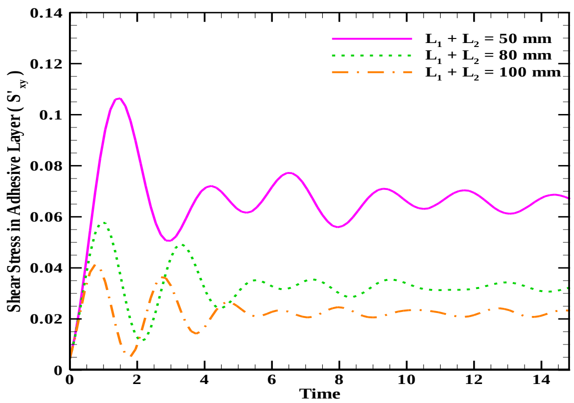

Fig.12
Diagram of effect of change in length of adhesive zone on the shear stress in adhesive.

After examining the effect of length change of the adhesive region on the joint, the aim was to evaluate the effect of changing the length of the non-adhesive region by considering the length of discontinuity and the adhesive constant on the load applied to the fibers which diagram is shown in Fig. 13.

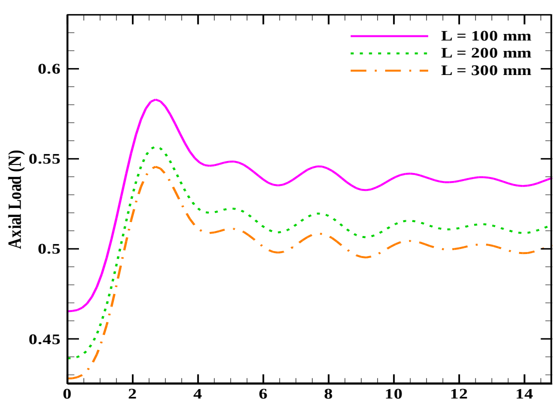

Fig.13
Diagram of the effect of the length change in non-adhesive area on the load applied to the fiber.

As shown in Fig. 13, increasing non-adhesive area length, the discontinuity area will be away from the edge of the applied load and increasing the distance of rupture place from the edge, the load applied to the fiber will be decreased.

Another parameter affecting the axial load applied to the fiber and shear stresses in the adhesive bonding of composite materials is the changing the spacing between fibers (matrix width) that in this sector, its effects have been studied. In Figs.14, 15 and 16, respectively the impact of the width change of matrix on the graph of applied distributed load on the fiber and shear stress in the matrix and adhesive for the case where the fibers fracture initiation is number thirteen is shown.

By increasing the width of matrix, the composite single layer width is increased. Since increasing the adhesive zone, the possibility of absorbing force applied to the plate is more, so it is expected that increasing the width of the matrix, the load applied to the fiber decreases, that Fig. 14 indicates this issue. With the increase of the adhesive region, fiber displacement is less as a result it is expected that shear stress generated in the matrix and adhesive reduces which Figs. 15 and 16 show it. Another point that is clear in Fig. 14 is that by increasing the width of the matrix, because of the increased surface of the adhesive area, the maximum amount of stress concentration factor and as a result shock imposed to the system is reduced after fiber breakage.

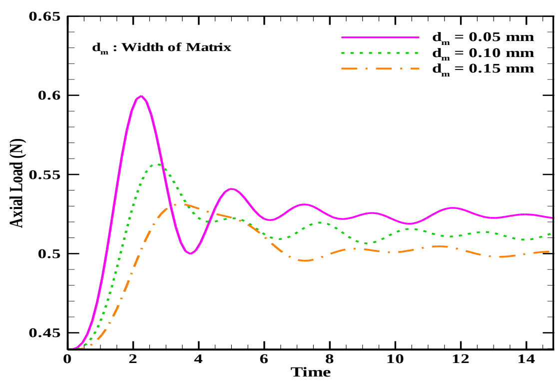

Fig.14
Diagram of effect of matrix width change on load applied to the fiber.

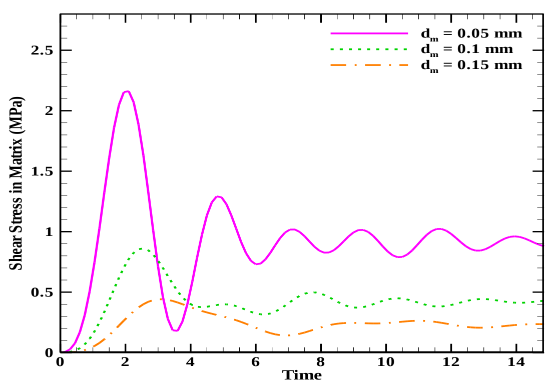

Fig.15
Diagram of the effect of changing the matrix width on the shear stress generated in the matrix.

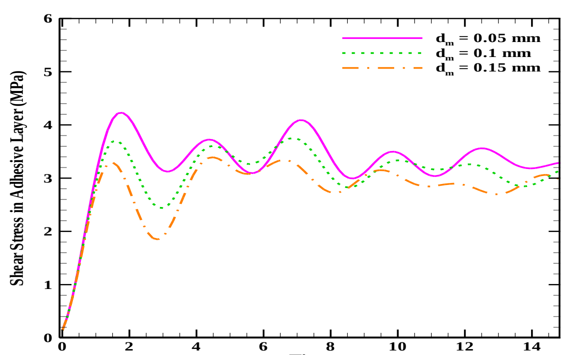

Fig.16
Diagram of the effect of changing the matrix width on the shear stress generated in the adhesive.

4 CONCLUSIONS

In this study, the distribution of transient stress induced by breakdown of fibers was investigated. The results of this research are:

- From the obtained diagrams of the results section it may be perceived that the dynamic effect of fiber breakage has been considerable in stress concentration and distribution of load in the composite material.
- In adhesive joint, a significant percentage of the force applied to the fiber is absorbed by the adhesive. As a result, the amount of axial load and the stress concentration factor in adhesive joint are too low than lamina.
- The amount of dynamic overshoot in single layer is more than adhesive joint. Due to the fact that in this joint, there is an adhesive layer, it is expected that by fiber breakage, the system faces less shock. With decreasing numerical distance between the static and dynamic stress concentration factor, dynamic overshoot will be reduced for adhesive joint than composite single layer.
- Whatever the starting location of the discontinuity displaced to the top edge and bottom edge the amount of load applied and as a result the stress concentration factor will also increase.
- In an adhesive joint, since by increasing the adhesive area, more length of fibers is in contact with the adhesive, so a greater amount of load applied to the fibers absorbed by the adhesive and thereby increasing the length of adhesive region, the amount of load applied to the fiber decreases. Due to the fact that the stress concentration factor is dependent to the fiber of tip of discontinuity place, thus reducing the load, this ratio is also reduced.
- With increasing non-adhesive area, rupture area will be far from the edge of applying load and with increasing the distance of discontinuity from the edge, the load applied to the fiber decreases.
- By increasing the width of the matrix, composite single layer width is increased. Since increasing the adhesive region, the absorption of applied forces to the lamina will be increased, so it is expected that increasing the width of the matrix, the load applied to the fiber decreases.

REFERENCES

[1] Mohseni Shakib M., 2011, *Mechanics of Composite Structures*, Imam-Hossein University, First Edition ,Tehran, Iran.

[2] Pickett A. K., Hollaway L., 1985, The Analysis of elastic adhesive stresses in bonded lap joints in FRP structures, *Composite Structures* **3**: 55-79.

[3] Nedele M. R., Wisnom M. R., 1994, Stress concentration factors around a broken fiber in a unidirectional carbon fiber-reinforced epoxy, *Institute of Structures and Deisgn* **25**: 549-557.

[4] Rajabi I., Rahimi F., Bakhshandeh K., 2007, Effects of single-Lap stress concentration in composite adhesive joints, *The 14th International Conference on Mechanic(ISME)*, Isfahan, Iran.

[5] Wang Z. Y., Wang L., Deng H., Tong J. W., Aymerich F., 2009, An investigation on strain/stress distribution around the overlap end of laminated composite single-lap joints, *Composite Structures* **89**: 589-595.

[6] Beylergil B., Cunedioglu Y., Aktas A., 2011, Experimental and numerical analysis of single lap composite joints with inter-adherend fibers, *Composite Part B* **42**: 1885-1896.

[7] Challita G., Othman R., 2012, Analytical model of the double-lap bonded joints response to harmonic loads, *European Journal of Mechanics A/Solids* **34**: 149-158.

[8] Mokhtari M., Madani K., Belhouari M., Touzain S., Feaugas X., Ratwani M., 2013, Effect of composite adherend properties on stresses in double lap bonded joints, *Materials and Design* **44**: 633-639.

[9] Mousavitabar H., 2010, *Stress Analysis of Composite Adhesive Joints*, M.Sc Thesis, Department of Mechanical Engineering, Shahid Chamran University, Ahwaz, Iran.

[10] Daniali M., 2012, *Investigation of Stress Concentration Due to Crack Existence in Composite Joint*, M.Sc Thesis, Department of Mechanical Engineering, Shahid Chamran University, Ahwaz, Iran.

[11] Hedgepeth J. M., 1961, *Stress Concentration in a Filamentary Structures*, Technical Note, D-882.

[12] Mirshekari E, 2010, *Transient Response of Stress Distributions in a Laminate Subjected to the Crack*, M.Sc Thesis, Department of Mechanical Engineering, Shahid Chamran University, Ahwaz, Iran.

[13] Chapra S.C., Canale R.P., 2010, *Numerical Method of Engineering*, McGraw-Hill, New York .

[14] Logan D.L., 2007, *A First Course in the Finite Element Method*, Thomson, University of Wisconsin-Platteville.